



**BNL-107375-2015-CP**

***Target and orbit feedback simulations of a muSR  
beamline at BNL***

**W. W. Mackay<sup>1</sup>, M. Blaskiewicz<sup>2</sup>, W. Fischer<sup>2</sup>, P. Pile<sup>2</sup>**

<sup>1</sup>25 Rhododendron Circle, Asheville, NC 28805 USA

<sup>2</sup>Brookhaven National Laboratory, Upton, NY 11973 USA

*Presented at the 6<sup>th</sup> International Particle Accelerator Conference (IPAC'15)*

Greater Richmond Convention Center, Richmond, VA 23219 USA

May 3 – 8, 2015

May 2015

**Collider Accelerator Department**

**Brookhaven National Laboratory**

**U.S. Department of Energy  
Office of Science, Office of Nuclear Physics**

Notice: This manuscript has been authored by employees of Brookhaven Science Associates, LLC under Contract No. DE-AC02-98CH10886/DE-SC0012704 with the U.S. Department of Energy. The publisher by accepting the manuscript for publication acknowledges that the United States Government retains a non-exclusive, paid-up, irrevocable, world-wide license to publish or reproduce the published form of this manuscript, or allow others to do so, for United States Government purposes.

This preprint is intended for publication in a journal or proceedings. Since changes may be made before publication, it may not be cited or reproduced without the author's permission.

## **DISCLAIMER**

This report was prepared as an account of work sponsored by an agency of the United States Government. Neither the United States Government nor any agency thereof, nor any of their employees, nor any of their contractors, subcontractors, or their employees, makes any warranty, express or implied, or assumes any legal liability or responsibility for the accuracy, completeness, or any third party's use or the results of such use of any information, apparatus, product, or process disclosed, or represents that its use would not infringe privately owned rights. Reference herein to any specific commercial product, process, or service by trade name, trademark, manufacturer, or otherwise, does not necessarily constitute or imply its endorsement, recommendation, or favoring by the United States Government or any agency thereof or its contractors or subcontractors. The views and opinions of authors expressed herein do not necessarily state or reflect those of the United States Government or any agency thereof.

# TARGET AND ORBIT FEEDBACK SIMULATIONS OF A $\mu$ SR BEAMLINE AT BNL\*

W. W. MacKay<sup>†</sup>, 25 Rhododendron Circle, Asheville, 28805  
M. Blaskiewicz<sup>‡</sup>, W. Fischer, and P. Pile, BNL, Upton, NY 11972

## Abstract

Well-polarized positive surface muons are a tool to measure the magnetic properties of materials since the precession rate of the spin can be determined from the observation of the positron directions when the muons decay. The use of the AGS complex at BNL has been explored for a  $\mu$ SR facility previously. Here we report simulations of a beamline with a target inside a solenoidal field, and of an orbit feedback system with single muon beam positioning monitors based on technology available today.

## INTRODUCTION

Muon spin rotation, relaxation and resonance ( $\mu$ SR) is a powerful technique for studying local magnetic fields in samples. When a positive pion decays at rest into a positive muon, the muon has a kinetic energy of 4.119 MeV (momentum 29.792 MeV/c) and its spin is opposite to its direction (negative helicity). If the pion decays near the surface of a target the resulting muons lose little energy, and the result is a beam of muons with a narrow energy distribution and almost 100% polarization. When these positive muons are implanted in matter with a magnetic field the muons precess at a rate proportional to the local field. When the muon decays the positron momentum is preferentially along the direction of the muon spin.

In this paper, we present improvements of our previous design for a surface muon beam line at BNL [1, 2] including optimization of the target and muon capture. Also we discuss the efficacy of a possible orbit feedback section to increase the density of the muon beam for experiments.

A beam of protons with kinetic energy 1.5 GeV will be extracted from the AGS (see Fig. 1) and focused onto a thin 0.5 mm wide target. An average intensity of  $10^{14}$  proton/s with a normalized rms emittance of  $8\pi \mu\text{m}$  is quite achievable from the AGS. Detailed parameters of the AGS and injector chain for  $\mu$ SR were presented previously [1].

The tracking code G4BEAMLINE [3] has been used for most simulations of the beam line in this paper.

## MUON TARGET AND CAPTURE

Pions which are produced and stop in the target will decay yielding muons which may exit the target if they are within 0.7 mm of the surface of the graphite target (see Fig. 2). Pions stopped any deeper in the target will produce muons which stop and decay inside the target lead-

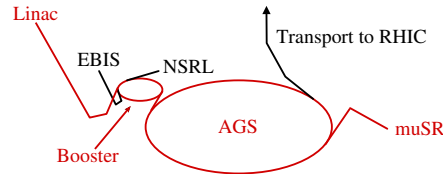


Figure 1: Schematic of the AGS complex with sections to be used for  $\mu$ SR shown in red.

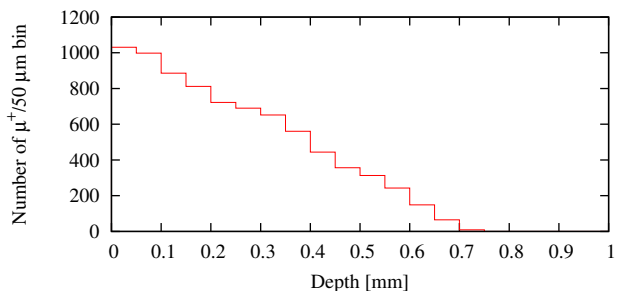


Figure 2: Number of  $\mu^+$  exiting the target from a uniform distribution of rest  $\pi^+$  placed inside a thick block of graphite. No  $\mu^+$  come from a depth greater than 0.7 mm.



Figure 3: Top view of target and proton beam. The proton beam is focused onto the middle of the narrow graphite  $200 \times 50 \times 0.5$  mm ( $l \times h \times w$ ) target.

ing to higher backgrounds and heating of the target and nearby beam-line elements. By making a long, horizontally thin target with the proton beam running down the length and having a waist focused at the center of the target, we can get surface muons from pions stopped near the surface with a minimum of background and heating. Fig. 3 shows a 200 mm long, 0.5 mm target, 50 mm high graphite target with a beam (noninteracting in the figure) having a  $\sigma_h^* = 0.25$  mm waist. For  $10^{14}$  protons/s simulations yield about  $15 \times 10^9 \mu^+$ /s 0.2 mm from the target's surface. Four times as many positrons are produced, but most are outside the momentum acceptance of the beam line.

To capture the muon beam, we use a decreasing field from four solenoids placed around the target as shown in Fig. 4. A scan of the capture efficiency versus the field of the upstream solenoid (-1) shown in Fig. 5 demonstrates that capture is more efficient with a negative slope to the axial field around the target. This is reminiscent of Adiabatic Matching Devices [6] used in positron linacs. Fig. 6 shows the momentum distributions of  $\mu^+$  and  $e^+$  at the exit of the solenoid 3.

\* Work supported by U.S. DOE under contract No DE-AC02-98CH10886 with the U.S. Department of Energy.

<sup>†</sup> wwmackay@charter.net

<sup>‡</sup> blaskiewicz@bnl.gov

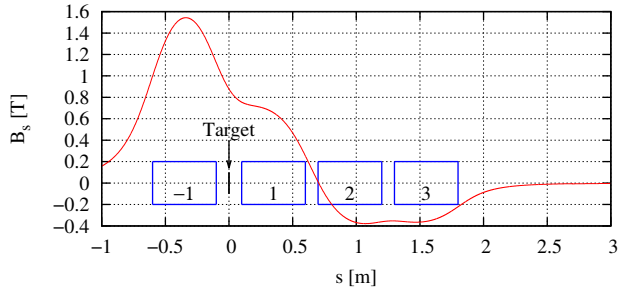


Figure 4: Layout of target and capture solenoids (blue). The proton beam hits the target placed between two solenoids (-1, 1) as shown with the target and proton beam perpendicular to the solenoid axis.  $\mu^+$  are captured by the three solenoids (1, 2, 3) to the right, with the upstream solenoid (-1) adding to the field at the target. The tapered capture fields of the solenoids along the axis are plotted in red. To decouple the magnetized muon beam, we require  $\int_0^\infty B_s ds = 0$ .

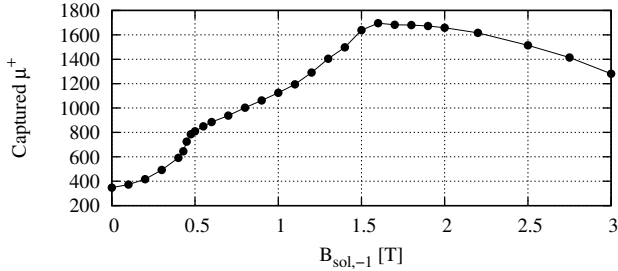


Figure 5: Fields scan of upstream solenoid (-1).

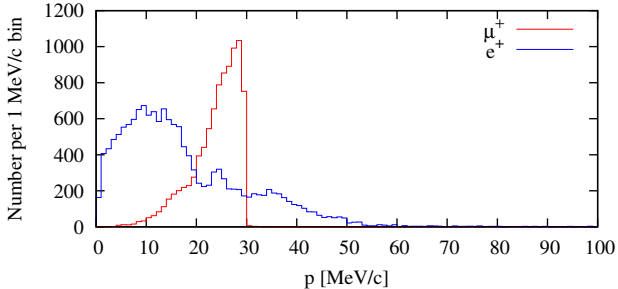


Figure 6: Momentum distribution of  $\mu^+$  and  $e^+$  just after solenoid 3 from a flux of  $1.77 \times 10^8$  protons.

## $\mu$ SR BEAM LINE WITHOUT FEEDBACK

After capture by the solenoids the surface muons are transported downstream through a series of three sector bends (see Fig. 7). The dipoles remove negative, neutral and off-momentum particles; any remaining pions decay before the end of the beam line. For focusing, we have replaced the earlier quadrupole doublets [1] with solenoid doublets to improve transport and shorten the beam line. Each pair of solenoid doublets are powered in series with opposite polarity to eliminate coupling. Following the first quadrupole triplet are two 1 m long separators (Wien filters) with vertical electric and horizontal magnetic fields to remove any remaining positrons from the muon beam. The separator voltage is about 338 kV with a transverse aperture  $h \times v$  :  $600 \times 200$  mm with the magnetic field

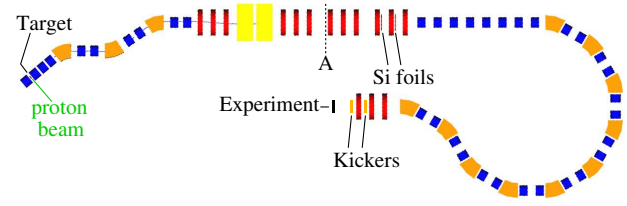


Figure 7: Layout of beam line in two parts: From left to dashed line A without orbit feedback. The distance from the target to line A is 19.83 m. The extension after the second triplet with the long arc provides delay for orbit feedback from thin Si detectors to steering correctors. The extended beam line has a length of 62.5 m from target to end. Beam line elements are colored as follows: solenoid (blue), dipole (orange), quadrupole (red), separator (yellow).

$B_x = -V_{\text{sep}}/hv_{\text{ref}}$  where  $v_{\text{ref}} = 0.256c$  is the velocity of a 28 MeV/c muon. The second quadrupole triplet then can focus the beam onto an experiment station at point A.

A flux of  $1.77 \times 10^8$  protons focused onto the target with  $\sigma_x^* = 0.25$  mm and  $\sigma_y^* = 1$  mm, produced 255  $\mu^+$  inside a circle of  $100 \text{ cm}^2$  which scales to a rate of 1.27 MHz/cm<sup>2</sup> for  $10^{14}$  protons/s. We estimate of peak temperature in the target assuming only radiative cooling to be about 2240 K. Scaling back the intensity to decrease target heating to 1600 K (without conduction or cooling) would give 0.33 MHz/cm<sup>2</sup> for  $2.6 \times 10^{13}$  protons/s, although higher temperatures could be acceptable [4, 5]. Further investigation of target cooling and somewhat larger  $\sigma_y^*$  remains to be done.

## EXTENDED BEAM LINE FOR FEEDBACK

To study the possibility of orbit feedback, we replace the experiment at A with a longer line as shown (Fig. 7) consisting of two more quadrupole triplets followed by four solenoid doublets, then five double bend achromats (DBA) and a final triplet for focusing the beam onto an experiment. With the low momentum beam, we use solenoid doublets to focus between dipoles rather than quadrupoles. Two thin Si foil detectors are placed after the 10th and 11th quadrupoles for position measurements. Two pairs (h and v) pulsed steering kickers are located fore and aft of the last quadrupole for orbit correction.

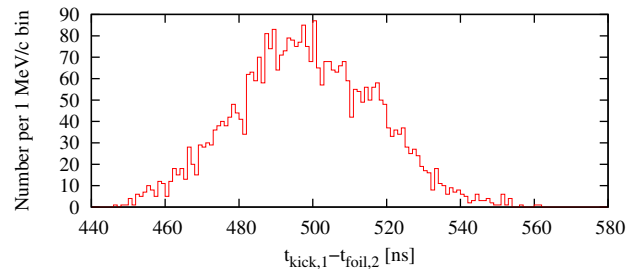


Figure 8: Distribution of muon time of flight from first foil to last kicker. The longest straight-line distance from foil to kicker is 6 m which corresponds to 30 ns for a 0.66 c cable.

Fig. 8 shows a distribution of time of flight from the first foil to the last kicker with a chord distance between foils and kickers of about 6 m. From this we see that about 100 ns of flattop is desirable for the kicker pulses with perhaps as much as 400 ns for signal processing. Since the feedback is to work on single muons, we would want a rate of no more than about 5–7 MHz at the foils. We reduced the muon rate by a factor of four by halving the separators' aperture in both transverse dimensions. A signal rate of 6.2 MHz corresponds to  $10^{13}$  protons/s.

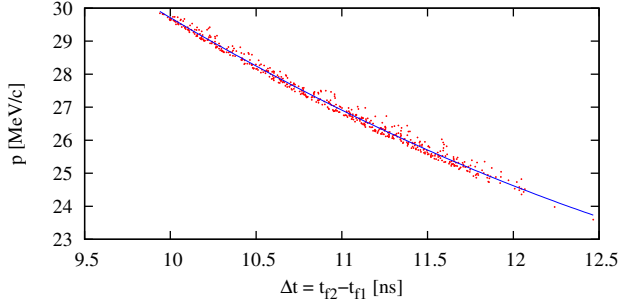


Figure 9: Momentum versus time of flight between the two foils. The blue curve is a parabolic fit to the data.

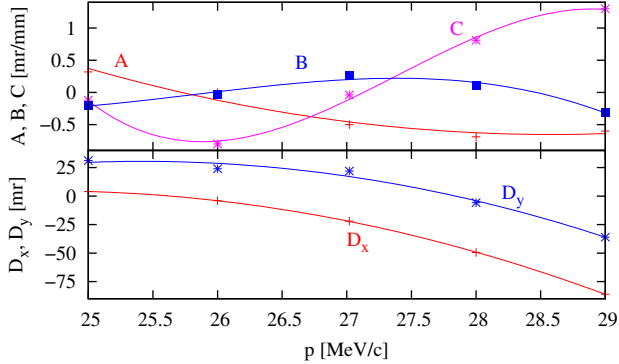


Figure 10: Fits to autotuning coefficients from tuning of monochromatic muon beams.  $A$ ,  $D_x$  and  $D_y$  are parabolic fits, and  $B$  and  $C$  are cubic fits.

We ran simulations with monochromatic muon beams at five different momenta to find coefficients of momentum dependent linear transformations for horizontal ( $x$ ) and vertical ( $y$ ) kicks at the two locations:

$$\theta_{x,k2} = A(p) x_{f1} + B(p) x_{f2} + D_x(p), \quad (1)$$

$$\theta_{y,k1} = C(p) y_{f1}, \quad \text{and} \quad \theta_{y,k2} = D_y(p), \quad (2)$$

where  $x_{f1}$ ,  $x_{f2}$ , and  $y_{f1}$  are the respective horizontal positions at foils 1 and 2 and vertical position at foil 1. Fig. 9 shows how the muon momentum  $p$  can be determined from the time of flight between the two foils. Momentum dependent fits to the five parameters are shown in Fig. 10.

Results from autotuning for different foil thicknesses are shown in Fig. 11 and summarized in Table 1 with rates scaled to  $10^{13}$  protons/s. Clearly the multiple scattering in foils thicker than  $10 \mu\text{m}$  will wash out orbit feedback.

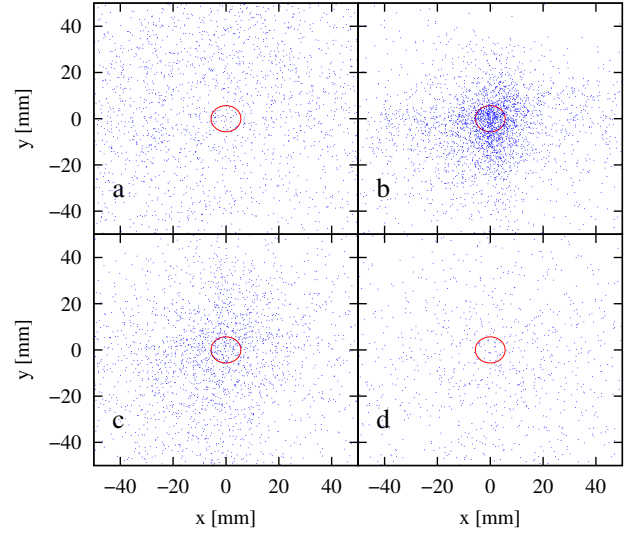


Figure 11: Muon distribution a) with no foils or autotuning, b) with autotuning and zero thickness foils, c) with  $10 \mu\text{m}$  foils and autotuning, d) with  $50 \mu\text{m}$  foils and autotuning. The red circles have an area of  $1 \text{ cm}^2$ .

Table 1:  $\mu^+$  Rates with Autotuning.

Thickness $\mu\text{m}$	$\# \mu^+$	Rate $\text{kHz/mm}^2$
$0^\dagger$	39	0.50
0	409	5.27
10	94	1.21
50	26	0.33

$^\dagger$  without autotuning.

## CONCLUSION

A 1.5 GeV kinetic energy proton beam focused with a  $\sigma_h^* = 0.25 \text{ mm}$  waist onto the center of a 200 mm long, 50 mm high, 0.5 mm wide graphite target can produce a large number of surface muons since muons from stopped pions can only exit the target from no deeper than 0.7 mm. For a flux of  $10^{14}$  protons/s, we expect about  $15 \times 10^9 \mu^+$  with  $p < 30 \text{ MeV}/c$  at 0.2 mm from the surface of the target and a flux of 0.33 to 1.27 MHz/cm<sup>2</sup> at the end of a 20 m long beam line depending on the target cooling. Target heating with different  $\sigma_y^*$  and conduction remains to be studied.

We also investigated the feasibility of single-particle orbit feedback with a large U-shaped turnaround to allow for signal processing from a pair of thin silicon foils for position measurements to pulsed steering magnets. The desired target flux would be about 40 kHz/mm<sup>2</sup>. An algorithm for increasing the final density of muons works in principle with zero-thickness foils to measure position and momentum via time-of-flight. Multiple scattering from foils of around  $10 \mu\text{m}$  can decrease or even eliminate any gain in density at an experiment. The additional requirement of single particle measurements at the foils further reduces the flux to an order of magnitude below the desired value even for zero-length foils with perfect time resolution.

## REFERENCES

- [1] M. Blaskiewicz et al., "Proposal for a  $\mu$ SR Facility at BNL", IPAC2013, Shanghai, THPWA052 (2013).
- [2] W. W. MacKay et al., " $\mu$ SR Beam Line Design Studies", BNL-103717-2013-IR, BNL, Upton, NY (2013).
- [3] T. Roberts, "G4beamline User's Guide 2.14", Muons Inc., (2012). (The Geant4 physics model selected was QGSP\_BERT 3.4.)
- [4] P. Thieberger, "Upper Limits for Sublimation Losses from Hot Carbon Targets in Vacuum and in Gasses", MUC-0186, BNL (2000).
- [5] J. R. Haines and C. C. Tsai, "Graphite Sublimation Tests for the Muon Collider/Neutrino Factory Target Development Program", ORNL/TM-2002/27, ORNL (2002).
- [6] R. Chehab et al., "An Adiabatic Matching Device for the Orsay Linear Positron Accelerator", IEEE Trans. on Nucl. Sci., NS-30, 2850 (1983).